Bone 51 (2012) 614–620

Contents lists available at SciVerse ScienceDirect

Bone

journal homepage: www.elsevier.com/locate/bone

Review

Variation in osteocytes morphology vs bone type in turtle shell and their exceptional preservation from the Jurassic to the present

Edwin A. Cadena *, Mary H. Schweitzer

Marine Earth and Atmospheric Sciences Department, North Carolina State University, Raleigh, NC 27695, USA

ARTICLE INFO

Article history:
Received 19 January 2012
Revised 3 May 2012
Accepted 4 May 2012
Available online 11 May 2012

Edited by: T. Jack Martin

Keywords:
Osteocyte morphology
Testudines
Cenozoic
Mesozoic
Exceptional preservation

ABSTRACT

Here we describe variations in osteocytes derived from each of the three bone layers that comprise the turtle shell. We examine osteocytes in bone from four extant turtle species to form a morphological 'baseline', and then compare these with morphologies of osteocytes preserved in Cenozoic and Mesozoic fossils. Two different morphotypes of osteocytes are recognized: flattened-oblate osteocytes (FO osteocytes), which are particularly abundant in the internal cortex and lamellae of secondary osteons in cancellous bone, and stellate osteocytes (SO osteocytes), principally present in the interstitial lamellae between secondary osteons and external cortex. We show that the morphology of osteocytes in each of the three bone layers is conserved through ontogeny. We also demonstrate that these morphological variations are phylogenetically independent, as well as independent of the bone origin (intramembranous or endochondral). Preservation of microstructures consistent with osteocytes in the morphology in Cenozoic and Mesozoic fossil turtle bones appears to be common, and occurs in diverse diagenetic environments including marine, freshwater, and terrestrial deposits. These data have potential to illuminate aspects of turtle biology and evolution previously unapproachable, such as estimates of genome size of extinct species, differences in metabolic rates among different bones from a single individual, and potential function of osteocytes as capsules for preservation of ancient biomolecules.

Contents

Introduction

Bone is the result of phylogenetic, functional, and structural influences [1] evidenced in the hierarchical levels of bone tissue: macrostructure (cancellous and cortical bone), microstructure (Haversian systems, osteons, and lamellae), and nanostructure (mineral, collagen, and non-

* Corresponding author.
E-mail address: eacadena@ncsu.edu (E.A. Cadena).

8756-3282/$ – see front matter © 2012 Elsevier Inc. All rights reserved.
doi:10.1016/j.bone.2012.05.002

collagenous proteins) [2]. Of the three types of cells comprising bone, osteocytes are the most abundant, making up 95% of all cells in bone ([3] and references therein), yet little is known of osteocyte biology and function. Recent studies have begun to elucidate the role of osteocytes in bone formation, bone function, bone maintenance and bone pathology [4–12], but many questions regarding the fundamental biology of these cells remain. Issues that are still poorly understood include: 1) the potential variation in the morphology of osteocytes in bones with different origins (intramembranous vs endochondral) and their different roles in vertebrate body plans, (e.g., do osteocytes function differently in long bones vs bony flat plates); 2) what temporal limits exist on osteocyte preservation in the bony matrix, and whether preservation is dependent on taxon, bone type, geologic time, depositional environment or other factors; and 3) if these cells persist and can be shown to be endogenous to the organisms, can chemical/molecular analyses of these remnants shed light on the physiology, phylogeny, and/or ecology of extinct organisms across geological time. Turtles are an ideal organism to inform on these issues, because their bony shell is unique among vertebrates, in that their carapace is endochondral in origin, while the plastron has an intramembranous origin [13] (see Graphical abstract). Additionally, their shell consists of bones with three well differentiated bone types or layers [14], and a robust and continuous fossil record extending approximately up to 230 million years (Ma).

Osteocyte lacunae and associated lacunocanalicular network (LCN) have been described in many fossil specimens [15–17], including non-avian dinosaurs from the Late Cretaceous (80 Ma) of Mongolia. Two different morphs of these structures have been identified: flattened-oblate and stellate [18]. More recently, three dimensional osteocytes and blood vessel morphs have been isolated from the bone matrices of various Mesozoic (dinosaurs) and Cenozoic (mammals-birds) vertebrates [19,20], but an in-depth examination of turtle bone for such preservation has not been previously conducted.

Here we describe osteocytes from four extant turtle taxa: sea turtle *Caretta caretta* (Cryptodira, Chelonidae), box turtle *Terrapene carolina* (Cryptodira, Testudinidae), freshwater turtle *Trachemys scripta* (Cryptodira, Emydidae), and freshwater side-necked turtle *Podocnemis expansa* (Pleurodira, Podocnemididae). We then examine the preservation of osteocytes in Cenozoic and Mesozoic fossils closely related to these extant species, and describe morphological variation in osteocytes from each of the three layers of bone that forms the shell—external cortex (EC), cancellous bone (CB), and internal cortex (IC). Finally, we compare these morphologies with osteocytes recovered from long bones (femora and humeri).

Materials and methods

Sampling

Complete skeletons of each extant species were donated for research from the Amphibian and Herpetological collections from the North Carolina Museum of Natural Sciences. We studied carapace and plastron elements of *C. caretta, Tr. scripta*, and *P. expansa*, as well as the right femur of *T. carolina* and *C. caretta*. Specimens used for comparing osteocyte morphology are described in the caption of Fig. 4.

Bone histology

Eleven bone thin sections (Table 1) were taken following the procedure described in Ref. [21], briefly summarized here and applied for both fossil and extant bones. Bone fragments were embedded in Silmar resin (Fiber Glass Florida, Inc., Florida) and allowed to polymerize. Sections were cut with a Covington saw to an approximate thickness of 1.5 mm and adhered to glass microscope slides (Fisherfinest, 3″×1″×1 mm) with Loctite Heavy Duty epoxy. After drying, sections were ground with an EcoMet 4000 Grinder/Polisher to 60–150 μm (below this range the osteocytes generally are lost, leaving just the empty lacunae), polished with grit paper decreasing in coarseness from 120 to 4000, and examined and documented with a Zeiss Axioskop 2 plus biological microscope and a Zeiss Axioskop 40 petrographic polarizing microscope. Images were collected using Axiovision software package (version 4.7.0.0).

Table 1
Bone thin sections of extant and fossil turtles studied, and stored at the North Carolina State University Paleontology Lab collection (NCSUPL).

Geologic time/location	Thin section catalogue number/bone
Present/North Carolina USA	*Caretta caretta* NCSUPL32/right costal 4
Present/North Carolina USA	*Caretta caretta* NCSUPL51/left femur
Present/North Carolina USA	*Trachemys scripta* NCSUPL22/left costal 5
Present/North Carolina USA	*Terrapene carolina* NCSUPL23/left femur
Present/North Carolina USA	*Terrapene carolina* NCSUPL52/right costal 4
Present/Peru	*Podocnemis expansa* NCSUPL30/left costal 5
Early Miocene (~23 Ma)/Panama	*Rhinoclemmys* sp.—NCSUPL05/left costal 4
Campanian (~80 Ma)/Mongolia	*Mongolemys elegans* adult—NCSUPL02/left costal 4
Campanian (~80 Ma)/Mongolia	*Mongolemys elegans* juvenile—NCSUPL01/right costal 7
Campanian (~80 Ma)/Mongolia	*Mongolemys elegans* hatching—NCSUPL03/left hyoplastron
Campanian (~80 Ma)/Mongolia	*Mongolemys elegans* hatching—NCSUPL03/left costal 6

Isolation of osteocytes

For isolation of extant osteocytes, small pieces of bone (~1 cm^3) were first placed in 50 ml tubes with ethylenediaminetetraacetic acid (EDTA; 0.5 M pH 8.0, filtered using a 0.22 μm filter) and subjected to gentle agitation for at least 10 days, using a VWR Scientific 3-D rotator waver to remove the mineral phase. Slices (~2 mm thick) of demineralized bone were transferred to microcentrifuge tubes (2 ml). EDTA was exchanged with E-pure water through multiple (at least 10) rinses. After demineralization, bone slices were incubated with collagenase A (Clostridiopeptidase, external cortex lyophilizate) to selectively remove collagen while leaving other features intact. For digestion, 80 μl of enzyme was diluted to 2 ml with D-PBS buffer solution and incubated with bone slices at 37.5 °C for at least 24 h with gentle shaking, centrifuged for 4 min at 2000 rpm, and then rinsed 2 times with PBS buffer. PBS was removed with e-pure water and drops of 5 μl were placed in glass slide with marked circular spots, cover slipped, and observed with a Zeiss Axioskop 2 plus biological microscope-fluorescence filter, using a 63× oil immersion lens.

Isolation of fossil osteocytes was performed in laboratories dedicated to analyses of ancient samples at North Carolina State University. To avoid contamination, these lab facilities are isolated from areas used to examine extant tissues. Clean room garb is required and all solutions and equipment remain in this dedicated lab area, never contacting recent material. Bone fragments were placed in cell culture plates (Costar, 6 wells) and incubated for 20 days in EDTA (0.5 M pH 8.0, 0.22 μm filtered), with four changes of solution. After this prolonged demineralization, approximately 100 μl was deposited on a glass slide, cover slipped, observed and photographed using a Zeiss Axioskop 2 plus biological microscope (40× and 63× oil lens).

Results

Osteocyte morphology in turtles

Two morphologically distinct types of osteocytes can be identified in ground sections of extant and extinct turtle bone or in isolated osteocytes after demineralization of each of these morphs specifically associated with variations in bone tissue (Figs. 1–3). These two morphologies are also conserved through ontogeny for each bone type, and for both shell elements (carapace and plastron), as is supported

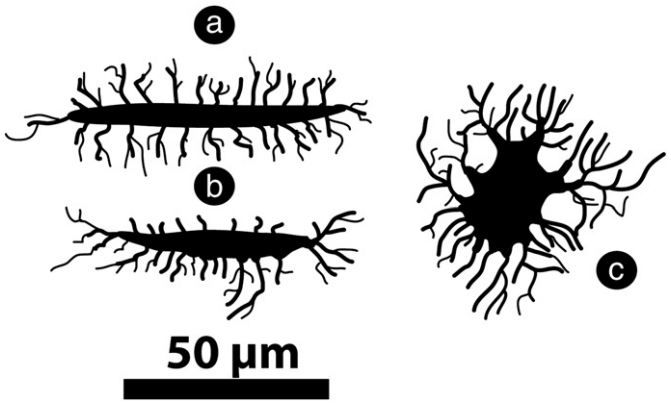

Fig. 1. Osteocyte morphotypes in turtle bone a. Flattened-oblate osteocyte (FO1 osteocytes) dominant morphotype of the internal cortex. b. Slightly wider and shorter variation of FO osteocytes (FO2), abundant in lamella of primary and secondary osteons. c. Stellate osteocytes (SO osteocytes) are the dominant morphotype of external cortices and regions between secondary osteons in cancellous bone.

from hatchling, juvenile, and adult specimens of *Mongolemys elegans* from the Late Cretaceous (80 Ma).

Flattened osteocytes (FO) (Figs. 1a–b)

Flattened (FO) osteocytes average 80–100 µm length and 5–15 µm width, and have long canaliculi processes (40–50 µm length) oriented perpendicular to the long axis of the osteocyte. FO1 osteocytes (Fig. 1a) are primarily found in the internal cortex of both carapace and plastron between layers of parallel-fibered lamellar bone, and occasionally in large secondary osteons. The filipodia may have secondary ramifications, but these are always shorter than the primary. The slightly shorter and wider variants of FO2 osteocytes (Fig. 1b) are abundant in the lamellae of primary and secondary osteons. These osteocytes may also exhibit more filipodia facing towards the Haversian canal at the center of the osteon, a pattern also observed in secondary osteons of equine bone [6].

Stellate osteocytes (SO) (Fig. 1c)

SO osteocytes are generally rounder (35–50 µm length; 30–40 µm width), some can be almost perfectly circular in shape. SO osteocytes are particularly abundant in the interstitial lamellae between osteons, where woven bone is also sometimes observed, and also in the external cortex of the carapace and plastron. The filipodia are more randomly distributed around the body of the osteocyte, and in most cases secondary and tertiary ramifications are present.

Osteocytes in ground sections

Both morphs of osteocytes described above are also observed in ground sections, indicating that demineralization does not affect the morphology or size of the osteocytes. Long bones of turtles, particularly the femur of extant turtles *C. caretta* and *T. carolina* are characterized by having both FO2 osteocytes in secondary osteons and SO osteocytes in interstitial lamellae between osteons of cancellous bone (Fig. 2a), and predominant SO osteocytes in cortical bone, where primary osteons are dominant (Fig. 2b). A ground section of costal bone (carapace) of the extant freshwater turtle *T. scripta* shows the abundance of FO1 osteocytes at the internal cortex (Fig. 2c), while FO2 and SO osteocytes are more prevalent in cancellous bone. FO1 osteocytes are more or less restricted in this area to the laminar bone of large secondary osteons (Fig. 2d), and the external cortex is characterized by SO osteocytes exclusively, which also shows abundant, densely distributed Sharpey's fibers (SF, Figs. 2e–f).

The same pattern of osteocyte morphology vs bone layer described above for the extant *T. scripta* is also observed in a costal bone from a hatchling of the fossil freshwater turtle *M. elegans* (Figs. 2g–i); and, as in *T. scripta*, Sharpey's fibers are abundant at the external cortex. From the same hatchling specimen of *M. elegans*, a ground section of the hyoplastron shows that the morphology and size of osteocytes for similar layer of bone (EC, CB, and IC) in both carapace and plastron are identical (Figs. 2j–l).

The morphology of osteocytes for the EC, CB, and IC is also independent of the lineages or taxa, as is shown by the ground section of an adult specimen of the fossil freshwater turtle *Rhinoclemmys* sp. from the Early Miocene (23 Ma) of Panama (Figs. 3a–f). In ground sections it was also possible to visualize the arrangement of the osteocyte-lacunae in fossils. That is the case for the hyoplastron from an adult specimen of *Mongolemy elegans* (Fig. 3g), where, in the IC, osteocyte bodies and their long-branchy filipodia occupy approximately 90% of the total bone volume. In some cases, connection of osteocytes via filipodia (Fig. 3h) can be observed directly.

Under polarized light, osteocytes from fossil turtles demonstrate isotropy, in contrast to the bone matrix. Figs. 3i–j, osteocytes in the CB of an adult specimen of the fossil *M. elegans*, is representative of this feature in all specimens observed.

Fig. 3k, shows the relationship between SO and FO1 osteocytes in the IC in a section of costal bone from an extant side-necked turtle (*P. expansa*) from South America. The arrangement consists of at least three layers of lamellar bone dominated by FO1 osteocytes with two layers of SO osteocytes between them (Fig. 3l), the layers with FO1 osteocytes are also darker than the layers with SO osteocytes.

Osteocytes in Mesozoic and Cenozoic turtles

Osteocytes in bone of Mesozoic and Cenozoic turtles are morphologically indistinguishable from osteocytes derived from two extant species, *T. scripta* (Figs. 4a–d) and *T. carolina* (Figs. 4e–f), although all fossil specimens show a red tint, while extant cells are virtually transparent. Osteocytes derived from the three layers of the bony shell of Mesozoic and Cenozoic turtles retain the same pattern of distribution as observed in ground sections. Fig. 4 shows: 1) Middle–Late Miocene (~13 Ma) osteocytes from a freshwater podocnemidid from Colombia (Figs. 4g–i); (2) Early Miocene (~23 Ma) freshwater-terrestrial *Rhinoclemys* sp., from Panama (Figs. 4j–l); (3) Early Eocene (~55 Ma) freshwater (indet.) podocnemidid turtle from Colombia (Fig. 4m); (4) Campanian (~80 Ma), freshwater *M. elegans* from Mongolia (Figs. 4n–w); (5) Campanian (~80 Ma), brackish bothremydid from North Carolina, USA (Figs. 4x–y); (6) Campanian (~80 Ma), brackish trionychid, from North Carolina, USA (Fig. 4z1); and (7) Late Jurassic (~150 Ma), freshwater-terrestrial *Annemis* sp., from Mongolia (Fig. 4z2). Occasionally, the cells demonstrate internal contents similar in morphology to nuclei (e.g. Figs. 4g, j, r, z2, arrows).

Discussion

Turtle osteocytes retain the typical stellate morphology mentioned by Ref. [22], also reported in non-avian dinosaurs [16] and other vertebrates [23,24]. One notable difference, however is that FO1 osteocytes (Fig. 1a) are more abundant in the turtle shell than in any other vertebrate, possibly due to the proximity of the internal cortex to the soft body of the turtle. The very flat shape of FO1 osteocytes observed in this layer of lamellar bone may be the result of the density and constrained orientation of collagen fibers [6], consistent with low rates in bone deposition. We hypothesize that the distinctive stratified arrangement between FO1 and SO osteocytes in the internal cortex of the extant species *P. expansa* (Figs. 3k–l) helps the bone to dissipate overload in the region dominated by SO osteocytes, and at the same time facilitates the beginning of bone resorption.

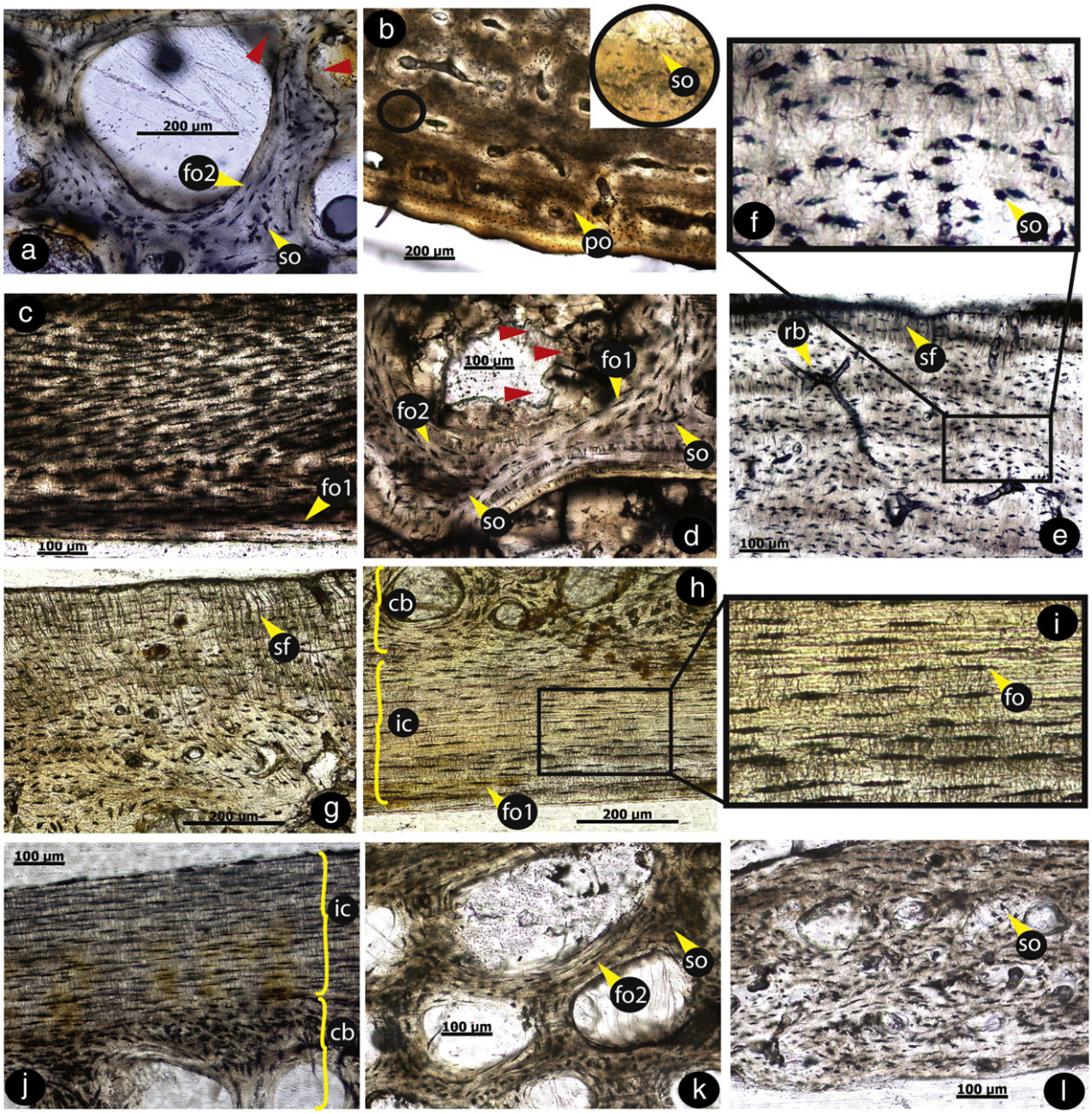

Fig. 2. Transmitted light images of ground sections of turtle bone. Extant sea turtle *Caretta caretta*, NCSUPL32/femur. a. Cancellous bone (CB), 20×, showing large bone resorption cavities in the cancellous bone around the central axis of the bone (red arrows), with FO2 osteocytes. b. Cortical bone, primary osteons are circular to slightly elongated in shape, matching the shape of the Haversian canals, and SO and FO2 osteocytes predominate, inset represents higher magnification view of region circled in b. c–e. Extant freshwater turtle (*Trachemys scripta*, NCSUPL22) left costal 5. c. Internal cortex (IC); d. CB (red arrows pointing resorption cavities); e. External cortex (EC); f. High magnification view or region outlined in e. EC. Fossil freshwater turtle *Mongolemys elegans* Campanian (~80 Ma), hatchling /NCSUPL03/left costal 6, g. EC; h. CB; i. higher magnification view of IC. Same fossil specimen, left hyoplastron, j. IC; k. CB; l. EC. Abbreviations: *FO1*, flattened-oblate osteocyte. *FO2*, flattened-oblate osteocyte, slightly wider and shorter than FO1. *SO*, stellate osteocyte. *po*, primary osteon. *rc*, resorption cavity. *sf*, Sharpey's fibers. *NCSUPL*, North Carolina State University Paleontology Lab microstructural bone collection.

The presence of lamellar woven bone in the regions with SO osteocytes could facilitate ossification. Bone formation is particularly important at the external cortex of both carapace and plastron, because this area of the turtle shell is most at risk of damage from environmental factors; particularly if the thin keratinous protective layer is removed by biotic or abiotic factors, (e.g. attack by predators, disease or infection, or abrasion).

The morphology of osteocytes in the turtle shell is independent of type of bone formation (endochondral (carapace) or intramembranous (plastron)), but rather is determined more by bone type (lamellar or woven), and arrangement of the three different bone layers EC, CB, and IC. Surprisingly, these morphological differences are independent of ontogenetic stage, as was observed in hatchling, juvenile, and adult specimens of the fossil turtle *M. elegans*. In addition, the morphology of osteocytes in turtles is independent of phylogeny, with a consistent pattern of distribution across taxa from both major groups of turtles; pleurodires or side-necked turtles (i.e. *P. expansa*) and cryptodires or hidden-necked turtles (i.e. *T. scripta*, *M. elegans*, and *Rhinoclemmys* sp.).

The data presented herein indicate that morphological preservation of osteocytes is not uncommon in Cenozoic and Mesozoic fossil turtle bone. Cellular preservation is independent of sedimentary environments, because osteocytes are observed in fossil turtles found in marine, freshwater, and terrestrial deposits. We hypothesize that rather than environmentally influenced, the morphological preservation of osteocytes

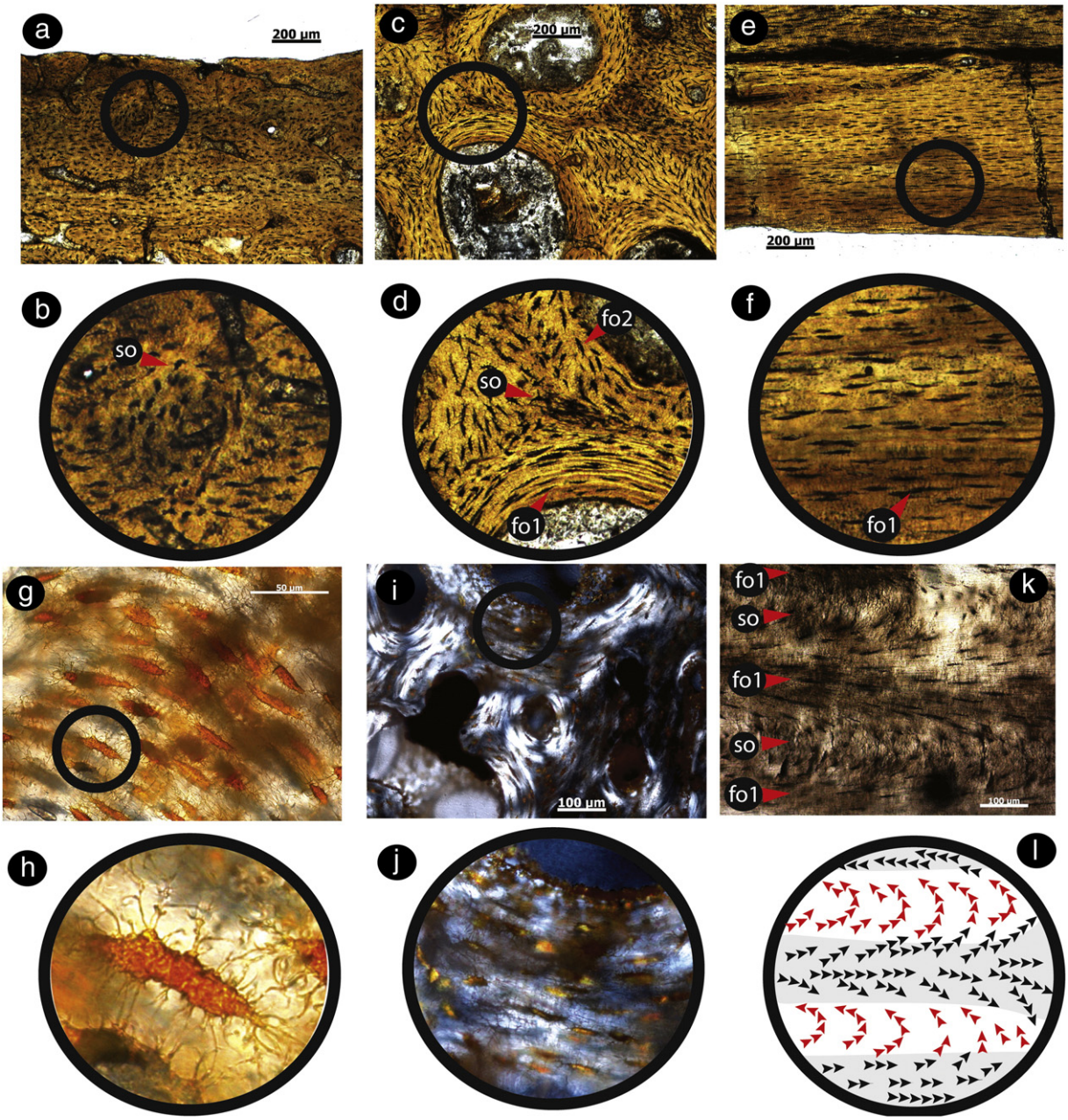

Fig. 3. *Rhinoclemmys* sp. Panama Canal/Early Miocene (~23 Ma), NCSUPL09/costal 5, a. EC, b. Close up for the area enclosed by the black circle in a, c. CB, d. close up for the area enclosed by the black circle in c, e. IC, f. Close up for the area enclosed by the black circle in e. g. FO2 osteocytes in *Mongolemys elegans* Mongolia/Campanian (~80 Ma)/NCSUPL02/left hyoplastron, adult specimen, CB 63× oil immersion, scale bar 50 µm. h. Close up for the area enclosed by the black circle in g, showing filipodia connections between osteocytes, and secondary branching of filipodia. i. Same specimen as in g, but different visual field, CB polarized light (PL)-20×. j. Close up for the area enclosed by the black circle in i, osteocytes keep the orange-brownish color from TL, while the mineral phase shows birefringence. k. Extant freshwater, side-necked turtle *Podocnemis expansa* NCSUPL30/costal 5, IC. l. Schematic diagram of the arrangement between FO1 and SO osteocytes in k, red arrows represent SO and their preferential orientation, black arrows show distribution of FO1, shaded areas approximate the boundaries between different layers of SO and FO1 Abbreviations: see Fig. 2 caption abbreviations.

in the fossil record may be attributed to their tridimensional encapsulation inside the bone mineral phase, which protects them from external or environmental factors promoting decay. Alternatively, preservation of osteocytes in the fossil record may be favored by high levels of intracellular osteocalcin [4], as this protein facilitates and promotes the binding of the mineral phase of bone [25] to the organic phase, increasing its preservation potential in the fossil record ([26] and reference therein). Chemical evidence supporting preservation and localization of osteocalcin to fossil osteocytes would support this hypothesis.

The best preserved osteocytes were derived from the shells of some of the older specimens, those from *M. elegans*, Late Cretaceous (Campanian, ~80 Ma) from Mongolia. These osteocytes demonstrate tridimensional morphology, and their lack of birefringence under polarized light (double refraction) is consistent with an organic source (Figs. 4i–j). Because most minerals demonstrate birefringence [27] and because common carbonate minerals would be chelated during EDTA incubation, the hypothesis of an osteocyte "mineral morph" is not consistent with the data, and instead, an organic origin is supported [20]. Although these data are insufficient to support the hypothesis that osteocytes from *Mongolemys* retain any original biomolecules, they do show that these osteocytes differ in composition from the mineral matrix in which they are embedded.

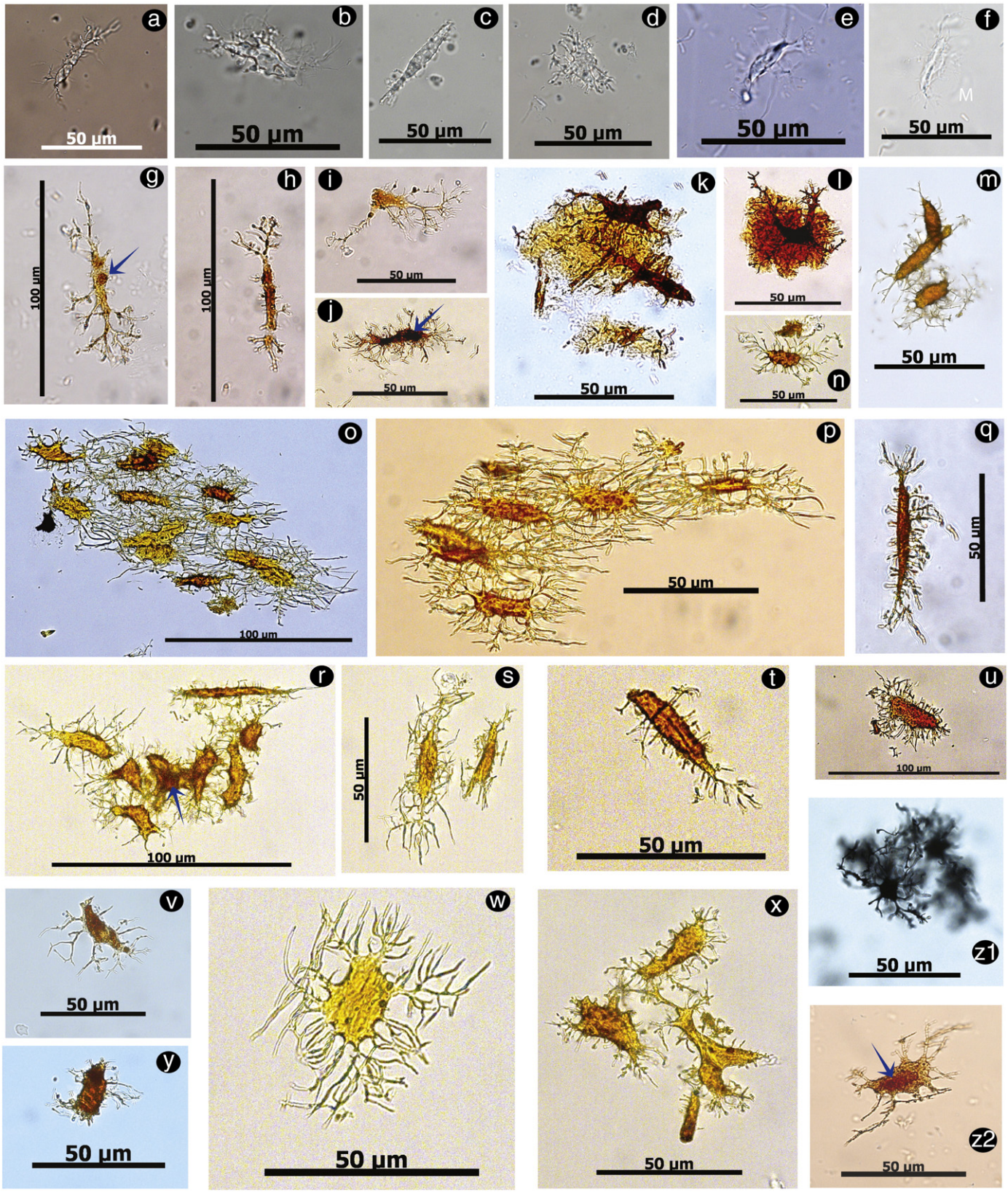

Fig. 4. Osteocytes isolated from extant and fossil turtles after demineralization and, in the case of extant material, post-digestion. All photographs were taken under transmitted light and 63× oil lens. a–d. Osteocytes from the extant freshwater turtle *Trachemys scripta*. e–f. Osteocytes from the extant terrestrial turtle *Terrapene carolina*. g–i. Middle–Late Miocene (ca.13 Ma) osteocytes from a freshwater podocnemidid from La Venta/Colombia. j–l. Early Miocene (ca. 23 Ma) freshwater-terrestrial *Rhinoclemmys* sp., from Panama. m. Early Eocene (ca. 55 Ma) freshwater podocnemidid indet turtle from Bogotá Fm/Colombia. n–w. Campanian (ca.80 Ma), freshwater *Mongolemys elegans* from Mongolia. x–y. Campanian (ca. 80 Ma), brackish water bothremydid from North Carolina, USA. z1. Campanian (ca.80 Ma), brackish water Trionychid, from North Carolina, USA. z2. Late Jurassic (ca.150 Ma), freshwater-terrestrial *Annemis* sp., from Mongolia. Blue arrows indicate internal structures similar to nuclei.

Current and future research in fossil turtle osteocytes

Ongoing efforts to characterize the chemical composition of these fossil osteocytes, using multiple analytical methods (e.g. high resolution mass spectrometry and *in situ* immunohistochemistry) are directed at the recovery of protein sequence from these specimens for phylogenetic analyses. Furthermore, Transmission Electron Microscopy (TEM) and focused ion beam/scanning electron microscopy (FIB/SEM) will discern whether organelles are preserved in some of these fossil osteocytes, yielding a better understanding of their 3D morphology and providing insights into possible preservation mechanisms.

We are also comparing the density of osteocytes (number osteocytes/mm^2 or mm^3 of bone) in the three different layers of the turtle shell, to quantitatively test the hypothesis that osteocyte density varies with bone type. These data will provide a test of the hypothesis advanced by Refs. [28,29], that osteocyte density is inversely proportional to body mass (g) and directly proportional to metabolic rate (kJ/day or hour). If our data support this hypothesis, we predict giant extinct turtles like *Stupendemys* (Miocene ~6 Ma) and *Archelon* (Late Cretaceous ~80 Ma) will exhibit a relatively low density of osteocytes, consistent with low metabolic rates, and that this will be unaffected by environmental differences (freshwater vs marine). We also predict that extant and fossils specimens, with similar body mass from the same genus of turtle, will exhibit similar osteocyte densities. If significant within-taxon variation is observed over time, it may indicate that other physiological, evolutionary, or environmental factors influence osteocyte density. A good candidate to test this hypothesis is the genus of freshwater turtle *Trachemys*, which has a fossil record that can be track for at least 10 Ma back from the Present.

Finally, the size of the lacunae in fossils once housing osteocytes has been used to establish genome size (C value) in vertebrates [30], supporting a positive correlation between C values and osteocyte-lacunae size [31]. This correlation has been used to propose genome size for extinct non-avian dinosaurs [32,33]. Turtles are an excellent group of animals to explore the osteocytes size-paleogenome size hypothesis, because some extant species for which the C-value is known, (e.g. *T. scripta* [34]), also have fossil record back in time for at least 5 Ma. Future research on this topic could shed light about rates of genomic divergence between lineages of turtles, morphology vs genome evolution in a deep time scale, and whether the most basal turtles differ from their potential ancestors with respect to genome size.

Acknowledgments

This work was supported by National Science Foundation grants OISE 0638810, EAR 0642528, and EAR 0824299, Geological Society of America Southeastern section Graduate Student Research Grant 2010 the Smithsonian Institution, the Panama Canal Authority, Mr. Mark Tupper, and SENACYT. Thanks to one anonymous reviewer for helpful comments. For access to samples of modern and fossil bones, thanks to B. Stuart and V. Schneider (North Carolina Museum of Natural Sciences, Raleigh, NC, USA). For support in lab preparations and microscopy thanks to T. Cleland and W. Zheng (North Carolina State University, Raleigh, NC, USA).

References

[1] Cubo J, Legendre P, de Ricqles A, Montes L, de Margerie E, Castanet J, et al. Phylogenetic, functional, and structural components of variation in bone growth rate of amniotes. Evol Dev 2008;10:217–27.
[2] Rho JY, Kunh-Spearing L, Zioupos P. Mechanical properties and the hierarchical structure of bone. Med Eng Phys 1998;20:92–102.
[3] Hirao M, Yamasaki N, Ando W, Tsuboi H, Myoui A, Yoshikawa H. Oxygen tension is an important mediator of the transformation of osteoblasts to osteocytes. J Bone Miner Metab 2007;25:266–76.
[4] Bonewald LF. The amazing osteocyte. J Bone Miner Res 2011;26:229–38.
[5] Lin Y, Xu S. AFM analysis of the lacunar–canalicular network in demineralized compact bone. J Microsc 2011;241:291–302.
[6] Kerschnitzki M, Wagermaier W, Roschger P, Seto J, Shahar R, Duda GN, et al. The organization of the osteocyte network mirrors the extracellular matrix orientation in bone. J Struct Biol 2011;173:303–11.
[7] Lu YB, Yuan BZ, Qin CL, Cao ZG, Xie YX, Dallas SL, et al. The biological function of DMP-1 in osteocyte maturation is mediated by its 57-kDa C-terminal fragment. J Bone Miner Res 2011;26:331–40.
[8] Sugawara Y, Ando R, Kamioka H, Ishihara Y, Honjo T, Kawanabe N, et al. The three-dimensional morphometry and cell–cell communication of the osteocyte network in chick and mouse embryonic calvaria. Calcif Tissue Int 2011;88:416–24.
[9] Schneider P, Meier M, Wepf R, Muller R. Serial FIB/SEM imaging for quantitative 3D assessment of the osteocyte lacuno-canalicular network. Bone 2011;49:304–11.
[10] Santos A, Bakker AD, Willems HM, Bravenboer N, Bronckers AL, Klein-Nulend J. Mechanical loading stimulates BMP7, but not BMP2, production by osteocytes. Calcif Tissue Int 2011;89:318–26.
[11] Kulkarni RN, Bakker AD, Gruber EV, Chae TD, Veldkamp JB, Klein-Nulend J, et al. MT1-MMP modulates the mechanosensitivity of osteocytes. Biochem Biophys Res Commun 2012;417:824–9.
[12] Atkins GJ, Findlay DM. Osteocyte regulation of bone mineral: a little give and take. Osteoporos Int in press, http://dx.doi.org/10.1007/s00198–012–1915-z.
[13] Kawashima-Ohya Y, Narita Y, Nagashima H, Usuda R, Kuratani S. Hepatocyte growth factor is crucial for development of the carapace in turtles. Evol Dev 2011;13:260–8.
[14] Scheyer TM. Comparative bone histology of the turtle shell (carapace and plastron): implications for turtle systematics, functional morphology and turtle origins. Bonn: Universitat Bonn; 2007. p. 125.
[15] Enlow DH, Brown SO. A comparatie histological study of fossil and recent bone tissues. Tex J Sci 1956;8:405–43.
[16] Pawlicki R. Morphological-differentiation of fossil dinosaur bone-cells—light, transmission electron-microscopic and scanning electron-microscopic studies. Acta Anat 1978;100:411–8.
[17] Pawlicki R, Dkorbel A, Kubiak H. Cells, collagen fibrils and vessels in dinosaur bone. Nature 1966;211:655–7.
[18] Pawlicki R. Metabolic pathways of the fossil dinosaur bones. 5. Morphological-differentiation of osteocyte lacunae and bone canaliculi and their significance in the system of extracellular communication. Folia Histochem Cytobiol 1985;23:165–74.
[19] Schweitzer MH, Wittmeyer JL, Horner JR. Soft tissue and cellular preservation in vertebrate skeletal elements from the Cretaceous to the present. Proc R Soc B Biol Sci 2007;274:183–97.
[20] Schweitzer MH. Soft tissue preservation in terrestrial Mesozoic vertebrates. Annu Rev Earth Planet Sci 2011;39:187–216.
[21] Schweitzer M, Organ C, Zheng WX, Asara J, Cleland T. Exceptional preservation of *Brachylophosaurus canadensis* (Campanian, Judith River Formation, USA). J Vertebr Paleontol 2008;28:139A.
[22] Klein-Nulend J, Nijweide PJ, Burger EH. Osteocyte and bone structure. Curr Osteoporos Rep 2003;1:5–10.
[23] Tanaka-Kamioka K, Kamioka H, Ris H, Lim SS. Osteocyte shape is dependent on actin filaments and osteocyte processes are unique actin-rich projections. J Bone Miner Res 1998;13:1555–68.
[24] Cao L, Moriishi T, Miyazaki T, Iimura T, Hamagaki M, Nakane A, et al. Comparative morphology of the osteocyte lacunocanalicular system in various vertebrates. J Bone Miner Metab 2011;29:662–70.
[25] Lee JS, Tung CH. Osteocalcin biomimic recognizes bone hydroxyapatite. Chembiochem 2011;12:1669–73.
[26] Buckley M, Howard S, Campbell S, Thomas-Oates J, Collins M. Distinguishing between archaeological sheep and goat bones using a single collagen peptide. J Archaeol Sci 2010;37:13–20.
[27] Nesse WD. Introduction to Optical Mineralogy. New York: Oxford; 2004.
[28] Bromage TG, Lacruz RS, Hogg R, Goldman HM, McFarlin SC, Warshaw J, et al. Lamellar bone is an incremental tissue reconciling enamel rhythms, body size, and organismal life history. Calcif Tissue Int 2009;84:388–404.
[29] Cullinane D. The role of osteocytes in bone regulation: mineral homeostasis versus mechanoreception. J Musculoskelet Neuronal Interact 2000;2:242–4.
[30] Gregory TR. The bigger the C-value, the larger the cell: genome size and red blood cell size in vertebrates. Blood Cells Mol Dis 2001;27:830–43.
[31] Montanari S, Brusatte SL, De Wolf W, Norell MA. Variation of osteocyte lacunae size within the tetrapod skeleton: implications for palaeogenomics. Biol Lett 2011;7:751–4.
[32] Organ CL, Shedlock AM, Meade A, Pagel M, Edwards SV. Origin of avian genome size and structure in non-avian dinosaurs. Nature 2007;446:180–4.
[33] Organ CL, Brusatte SL, Stein K. Sauropod dinosaurs evolved moderately sized genomes unrelated to body size. Proc Biol Sci 2009;276:4303–8.
[34] Kasai F, O'Brien PC, Ferguson-Smith MA. Reassessment of genome size in turtle and crocodile based on chromosome measurement by flow karyotyping: close similarity to chicken. Biol Lett in press, http://dx.doi.org/10.1098/rsbl.2012.0141.